NONLINEAR PROPAGATION OF NARROW PULSES OF OPTICAL RADIATION IN A SOLID-PARTICLE AEROSOL

D.S. Bobuchenko and V.K. Pustovalov

Belorussian Poly technical Institute, Minsk
Received August 7, 1989

The nonlinear propagation of narrow pulses of optical radiation in solid-particle aerosol is studied based on the numerical solution of a system of equations on a computer. The formation of nonstationary thermal and mass halos, which do not interact with one another, around the vaporizing aerosol particles which scatter the radiation is taken into account.

The nonlinear interaction of intense optical radiation with solid aerosol particles and the propagation of radiation in a solid-particle aerosol have been widely studied in the last few years both experimentally and theoretically.[1,2] The interaction of intense optical radiation with metallic aerosol particles is of special interest. This is necessary for solving problems in the nonlinear optical sounding of the dust-filled atmosphere of industrial cities, laser diagnostics of two-phase flows, the propagation of optical radiation in a solid-particle aerosol, etc. Metallic particles, which absorb and scatter the radiation, melt, and are vaporized, attenuate the radiation and appreciably affect the spatial-temporal distribution of the radiation intensity, the energy balance of the interaction process, etc. Experimental investigations of the interaction of intense radiation with dispersed metallic particles have been performed in Ref. 3. In Refs. 4 and 5 the heating, melting, and vaporization of a single metallic aerosol particle in a gas under the action of intense radiation were studied theoretically under conditions of diffusive-convective heat and mass transfer, taking into account the real temperature dependences of the thermophysical and optical parameters, the transfer coefficients, etc. It is of great interest to study theoretically the nonlinear propagation of narrow pulses of optical radiation in a metallic aerosol with characteristic particle radii ~ -10 μm based on the model for a single particle[4,5] taking into account heating, melting, and vaporization of the particles by the radiation.

We shall study the nonlinear propagation of pulses of radiation through a polydispersed metallic aerosol with a starting particle number density N_0 and particle-size distribution function $f_0(r_0)$. We shall confine our attention to values of the radiation intensity I_0 (the energy density E_0) for which optical breakdown of the aerosol and plasma formation do not occur, but intense heating and vaporization of the particles are possible. The metallic particles are in an inert gaseous medium, i.e., oxidation, inflammation, and combustion of the metallic particles under the action of the radiation[5] can be ignored. We shall study the case of the propagation of a narrow pulse of radiation, when the pulse width t_p satisfies the conditions

$$t_c, t_{TO}, t_T, t_D \ll t_p \ll t_{OVT}, t_{OVD} \qquad (1)$$

where $t_c \approx \frac{r_0}{C_s}$ is the characteristic pressure equalization time near the particle; r_0 is the radius of the particle; C_s is the velocity of sound in the gas; $t_{TO} \approx \frac{r_0^2}{4\chi_0}$ is the characteristic to equalization time of the temperature profile of the particle; χ_0 is the thermal diffusivity of the particle material; $t_T \approx \frac{r_0^2}{4\chi}$, $t_D \approx \frac{r_0^2}{4D}$, are the characteristic times over which the quasistationary external temperature and density fields are established in the vicinity of the particle; $t_{ovD} \approx N_0^{-2/3}/4D$ are the characteristic times during which the thermal and diffusion halos from neighboring particles overlap;[1] χ is the thermal diffusivity of the gas; and, D is the diffusion coefficient in the gas.

The system of equations describing the nonlinear propagation of radiation pulses with width t_p, satisfying the conditions (1), and wavelength λ along the x axis in a polydispersed solid-particle aerosol has the following form, taking into account the vaporization of the particles in the approximation of a uniform temperature T_0 over the volume of the particles:

$$\frac{\partial I}{\partial x} = (\alpha_0 + \alpha_{hp} + \alpha_m) I = 0,$$

where

$$\alpha_0 = \pi N_0 \int_0^\infty r_0^2 [K_a(r_0) + K_s(r_0)] f(r_0) dr_0 \qquad (2)$$

$$\alpha_{hp} = N_0 \int_0^\infty S_{hp} f(r_0) dr_0;$$

$$S_{hp} = \pi k^4 \int_0^\pi (1 + \cos^2\theta)\sin\theta \, d\theta \times$$

$$\times \left[\int_{r_0}^{r_c} dr r^2 (n^2 - n_0^2) \frac{\sin\left[2kr \sin\frac{\theta}{2}\right]}{2kr \sin\frac{\theta}{2}} \right]^2;$$

$$\rho_0 V_0 c_0 \frac{\partial T_0}{\partial t} = \frac{1}{4} I K_a S_0 - \bar{j}_\varepsilon S_0; \tag{3}$$

$$\frac{d(\rho_0 V_0)}{dt} = -\bar{j}_m S_0; \tag{4}$$

$$\frac{\partial f}{\partial t} + \frac{\partial}{\partial r_0}\left[f \frac{\partial r_0}{\partial t} \right] = 0. \tag{5}$$

For $r \geq r_0$

$$c\rho \frac{\partial T}{\partial t} = \frac{1}{r^2} \frac{\partial}{\partial r}\left[r^2 \chi \frac{\partial T}{\partial r} \right]; \tag{6}$$

$$\frac{\partial \rho_1}{\partial t} = \frac{1}{r^2} \frac{\partial}{\partial r}\left[r^2 \rho D \frac{\partial c_1}{\partial r} \right]; \tag{7}$$

$$p = R_g \rho T = p_\infty = \text{const}, \tag{8}$$

where I is the intensity of the radiation; a_0, a_h, and a_m are, respectively, the radiation attenuation coefficients of the particles, the thermal halos around the particles, and the gas (since $a_m \ll a_0$, in what follows we shall neglect a_m); K_a, K_s, and $K_e = K_a + K_s$ are the absorption, scattering, and extinction efficiency factors of a particle with an instantaneous radius r_0; $f(r_0)$ is the particle-size distribution function of a polydispersed aerosol; $\int_0^\infty f(r_0)\partial r_0 = 1$; n and n_0 are, respectively, the instantaneous and initial values of the index of refraction of the gas phase; $k = \frac{2\pi}{\lambda}$; r is the radius in a spherical coordinate system whose origin lies at the center of the particle; ρ_0 and C_0 are the density and heat capacity of the particle material; t is the time; $V_0 = 4/3\pi r_0^2$; $S_0 = 4\pi r_0^2$; $\bar{j}_m$ and $\bar{j}_\varepsilon$ are, respectively, the mass and energy flux densities from the surface of the particle, vaporizing in a diffusive-convective regime, taking into account the jumps in the density of the vapor and the real temperature dependences of the transfer coefficients;[4,5] C and $\rho = \rho_1 + \rho_2$ are the heat capacity and density of the vapor-gas mixture; ρ_1 and ρ_2 are the density of the vapor and the surrounding gas; $C_1 = \rho_1/\rho$ is the concentration of the vapor; κ is the thermal conductivity; P is the pressure; R_g is the gas constant; and P_∞ is the initial pressure of the gas.

The system of equations (2)–(8) includes the equation of radiation transfer in the approximation of single scattering by particles and the thermal halos around the particles (2), the equations of energy balance (3) and mass balance (4) for a single particle, the equation (5) describing the change in the particle-size distribution function owing to vaporization, the heat-conduct ion and diffusion equations (6) and (7), describing the distribution of the temperature T and the vapor density ρ_1 in the thermal and mass halo around the particle, and the equation expressing the constancy of the pressure of the vapor-gas mixture (8). The initial and boundary conditions for the system (2)—(8) are as follows:

$$\begin{aligned}
&\alpha_0(x, t = 0) = \alpha_\infty; \ \alpha_{hp}(x, t = 0) = 0; \\
&T_0(x, t = 0) = T_\infty; \ T(r, t = 0) = T_\infty; \\
&r_0(x, t =) = r_\infty; \ \rho_1(r, t = 0) = 0; \\
&T(r = r_c, t) = T_\infty; \ \rho_1(r = r_c, t) = 0,
\end{aligned} \tag{9}$$

where α_∞, T_∞, and r_∞ are the initial values of the corresponding parameters and $r_c = \frac{1}{2} N_0^{-1/3}$ is one-half the distance between the centers of neighboring particles.

The temperature dependences of the thermal conductivity κ and the diffusion constant D were determined in the form $\kappa = \kappa_\infty (T/T_\infty)^{0.75}$; $D = D_\infty (T/T_\infty)^{1.75}$; $\kappa_\infty = \kappa(T_\infty)$; $D_\infty = D(T_\infty)$ (Ref. 6). The index of refraction of the vapor-gas mixture around separate particles is determined by the relation

$$n = 1 + \frac{2\pi\alpha_1}{m_1} \rho_1 + \frac{2\pi\alpha_2}{m_2} \rho_2, \tag{10}$$

where α_1, α_2 and m_1, m_2 are, respectively, the polarizabilities and masses of the atoms of the vapor and gas.[7,8]

The thermal and mass halo makes an appreciable contribution to the attenuation of the radiation, if the characteristic radius of the halo r_h is much greater than the particle radius r_0. In this case, the main mechanisms of formation of the thermal and mass halo are diffusion and heat condition, since the velocity of the convective motion is significant only for determining $\bar{j}_m$ and $\bar{j}_\varepsilon$ at the surface of the particle and drops rapidly for $r \gg r_0$. In all variants calculated there is no interaction of the thermal and mass halos from neighboring particles during the pulse, and the interaction in S_h and in Eqs. (6) and (7) is performed up to r_c.

We shall employ below the dimensionless spatial variable ξ, related with the spatial variable x by the

equation: $x = 1.274 \cdot 10^6\ \xi/N_0$, cm. In this problem the particle number density N_0 enters only this relation between x and ξ, and all computational results presented below can be converted to different values of $N_0 < 10^{-3}$ cm^{-3}, which satisfy the condition for noninteracting thermal and mass halos from neighboring particles.

We shall examine some computational results for the interaction of an optical pulse with $\lambda = 10.6$ μm, $t_p = 2 \cdot 10^{-3}$ s, square time dependence, and energy density $E_0 = 6 \cdot 10^3$ J/cm^2 with a layer of polydispersed aluminum particles in helium at atmospheric pressure. The values of the parameters are taken from Refs. 6–9. The polydispersity of the particles is taken into account in the multigroup approximation. The following initial radii r_{01} and weights of the particle groups f_{01} were used: 15, 20, 25, 30, and 35 μm and 0.1, 0.2, 0.4, 0.2, and 0.1, respectively. We shall present estimates of the characteristic heat-transfer times for a particle with $r_0 = 25$ μm for $N_0 = 1 \cdot 10^2$ cm^{-3}; $t_{TO} \sim 1.5 \cdot 10^{-6}$ s; $t_p \sim 2.5 \cdot 10^{-6}$ s; $t_T \sim 7.8 \cdot 10^{-6}$ s; $t_c \sim 7.5 \cdot 10^{-8}$ s; $t_{ovDT} \sim 1.9 \cdot 10^{-2}$ s; $t_{ovT} \sim 1.1 \cdot 10^{-2}$ s. In this case with $t_p = 2 \cdot 10^{-3}$ s the condition (1) is satisfied. We note that the distribution of heat sources as a result of the absorption of radiation with $\lambda = 10.6$ μm in Al particles is substantially nonuniform.[10] However numerical calculations of the heating, melting, and vaporization of Al particles with $r_0 \sim 10$–100 μm for $t_p = 10^{-5}$ s using heat sources[10] showed that the temperature inside the particles equalizes over a time $\sim 10^{-5}$– 10^{-6} s (this agrees with the estimate presented for t_{TO}) and the approximation of a uniform temperature inside a particle can be employed. It should also be noted that under real conditions Al particles usually have an Al_2O_3 oxide film with thickness $h \sim 0.1$–0.01 μm on the surface. The presence of the oxide film can appreciable change the optical characteristics of Al. Thus, for example, for $\lambda = 10.6$ μm and $r_0 = 25$ μm the computed values of the efficiency factors K_a and K_s for $T_0 = T\infty = 300$ K for the cases without and with an oxide film with $h = 0.1$ μm equal, respectively, $K_a = 6.09 \cdot 10^{-2}$, $K = 2.015$ and $K_a = 8.72 \cdot 10^{-2}$, $K_s = 1.93$ for the optical parameters of Al and Al_2O_3 given In Refs. 11 and 12. The effect of the temperature dependence of the optical constants of Al and Al_2O_3 (Refs. 11 and 12) and the presence of an oxide film with $h = 0.1$ μm on K_a and K_s in the process of heating and vaporization of a particle by the radiation was taken into account. In the case when a particle melts at a temperature $T_0 = T_{melt} = 933.6$ K the oxide film cracks and breaks away. Therefore for $T_0 > T_{melt}$ the oxide film has no effect on the heating and vaporization of the particle, and for this reason it is ignored.

Figure 1 shows the time dependences of T_0 and r_0 for particles with radius $r_\infty = 15$, 25 and 35 μm, located on the boundary of the aerosol at $\xi = 0$. The particles absorb energy from the moment they are exposed to the radiation, they heat up, and at $T_0 = T_{melt} = 933.6$ K they melt over some time interval. Since the density of liquid aluminum (2.35 g/cm^3) is lower than that of solid aluminum (2.7 g/cm^3),[9] the radius of the particle after melting, taking into account the mass of the particle, increases to $r_0 \approx 1.05\ r_\infty$. The particle temperatures subsequently increase and reach the maximum values T_{max}, at which the energy released in a particle as a result of absorption of radiation is balanced by energy losses owing to intense vaporization of the particles and heat transfer from the particles. In the process of vaporization the radius of the particles r_0 decreases and T_0 decreases with time as a result of the fact that the energy losses from a particle exceed the energy released in the particle. For $r_0 \le 1$–2 μm the efficiency of the absorption of radiation by a particle drops sharply, which results in more rapid decrease of T_0 and slowing down of the vaporization of the particle.

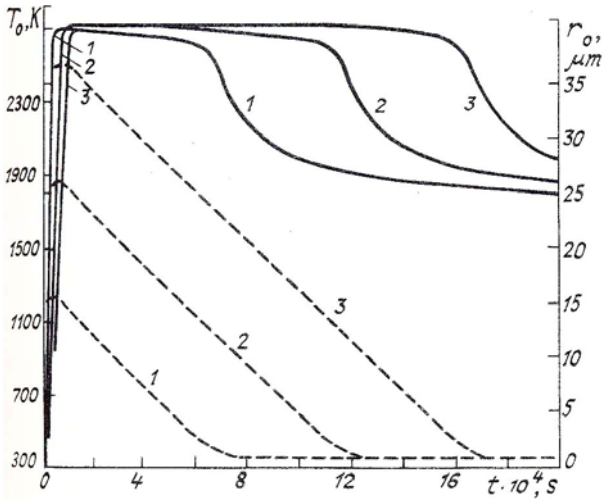

FIG. 1. The time dependences of the temperature T_0 (solid lines) and radius of AL particles r_0 (dashed lines) for $r_\infty = 15$ (1), 25 (2) and 35 (3) μm with $\xi = 0$ for a pulse of radiation with $\lambda = 10.6$ μm, $t_p = 2 \cdot 10^{-3}$ s, and $E_0 = 6 \cdot 10^3$ J/cm^2.

Heat exchange between the heated particles and the surrounding gas owing to nonlinear heat conduction occurs from the moment when the radiation pulse starts to Interact with the aerosol. In the process a spherically symmetric (based on the assumptions made) nonstationary temperature distribution $T(r, t)$ – the thermal halo – arises around the particle. In addition, from the moment that intense vaporization of the particle starts a nonstationary distribution of the vapor density ρ_1 arises around the particle as a result of the flow of vapor from the surface of the particle and diffusion of the vapor into the surrounding gas. Since the index of refraction of the two-component vapor-gas medium depends on T and ρ_1 (10) this results in the appearance of optical nonuniformity around the particle (thermal and mass halo), giving rise to additional scattering of the radiation. We note that the effect of

nonstationary acoustic and thermal halos on the attenuation of narrow pulses of intense radiation propagating in a solid-particle aerosol was studied theoretically.[1,2] In Refs. 13 and 14 the attenuation of radiation by thermal and mass halos arising when radiation interacts with a soot aerosol was studied in the approximation of quasistationary distributions $T(r)$ and $\rho_1(r)$ and the radius of the halo was determined based on the law of conservation of the energy removed from the particle. In the process, essentially only the thermal halos were studied, since it was assumed that the composition of the gas mixture around the particles is close to the starting composition.

In this paper the nonstationary two-component thermal and mass halos, forming around particles exchanging heat and mass with the a gaseous medium by the mechanisms of diffusion and heat conduction, were studied in the Rayleigh-Gans approximation $|n - n_0| \ll 1$. Figure 2 shows for several times the distributions of T, $c_1 = \rho_1/\rho$, and $n - 1$ as a function of r around a particle located on the boundary of an aerosol. The index of refraction n of the medium for a two-component thermal and mass halo around particles depends as follows on ρ_1 and T (see Eqs. (8) and (10)): $n - 1 = a_1\rho_1 + a_2/T$:

$$a_1 = 2\pi\left(\frac{\alpha_1}{m_1} - \frac{\alpha_2}{m_2}\right) + \frac{2\pi\alpha_2(R_2 - R_1)}{m_2R_2}, \quad a_2 = \frac{2\pi\alpha_2 P_\infty}{mR};$$

$R_{g_{22}} = c_1R_1 + (1 - c_1)R_2$, where R_1 and R_2 are the gas constants of the vapor and the surrounding gas. The distributions $T(r, t)$, $\rho_1(r, t)$, $c_1(r, t)$ depend on the instantaneous values of the radius r_1 and temperature T_0 of the particle and decrease to their initial values as r increases. The decrease in ρ_1 and T as r increases, taking into account the dependence of $n - 1$ on ρ_1 and T, results in nonmonotonic behavior of $n - 1$ as a function of r — a maximum appears at some distance from the particle. As $r \to r_s$ the value of $n - 1$ approaches $n_0 - 1 = 3.18 \cdot 10^{-1}$ for the starting gas. In addition, as time passes there arises, in addition to spatial regions in which $n - 1 > n_0 - 1$, a spatial region in which $n - 1 < n_0 - 1$ (see Fig. 2). The appearance of spatial regions with $n < n_0$ and with $n > n_0$, owing to the mutually compensating contribution of ρ_1 and T to thermal and mass halo, results after integration over r in S_h in a decrease of the integrand and the values of S_h and α_h with the passage of time. Taking into account the contribution of the distributions of ρ_1 and T over r in the nonstationary thermal and mass halo reduces S_h and α_h below their values with a purely thermal halo. Thus when the radiation interacts with solid particles α_h at first increases and then decreases with the passage of time. An analogous picture of the appearance and development of thermal and mass halos is observed for all particles in the aerosol layer (see Fig. 4.)

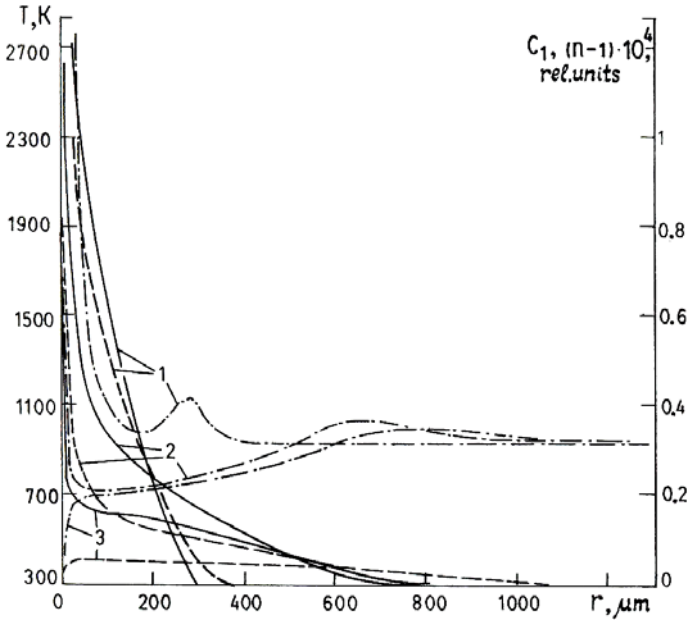

FIG. 2. The distribution of T (solid lines), the vapor concentration c_1 (dashed lines), and the index of refraction of the medium $n - 1$ (dot-dashed lines) as a function of r around a particle with $r_\infty = 25$ μm with $\xi = 0$ at different times (s): $1.5 \cdot 10^{-4}$ (1), $1.05 \cdot 10^{-3}$ (2), $1.5 \cdot 10^{-3}$ (3).

The quasi stationary distributions T, c_1, and $n - 1$ as a function of r (Ref. 5) and the values of S_h and α_h were also calculated. They differ significantly by as much as an order of magnitude, from the nonstationary distributions of T, c_1, and $n - 1$ and the corresponding values of S_h and α_h; this indicates that the formation of the thermal and mass halos is an substantially nonstationary process. In addition, the decrease in T_0 in the process of intense vaporization of a particle results with the passage of time in a sharp drop of ρ_1 at

the surface of the particle and the appearance of a profile $\rho_1(r)$ with a maximum at some distance from the particle (see Fig. 2). This fact cannot be taken into account by the quasistationary distribution $\rho_1(r)$. Therefore the possibility of calculating S_h and α_h based on the quasistationary distributions of the parameters[13,14] is substantially limited and must be determined in each specific case.

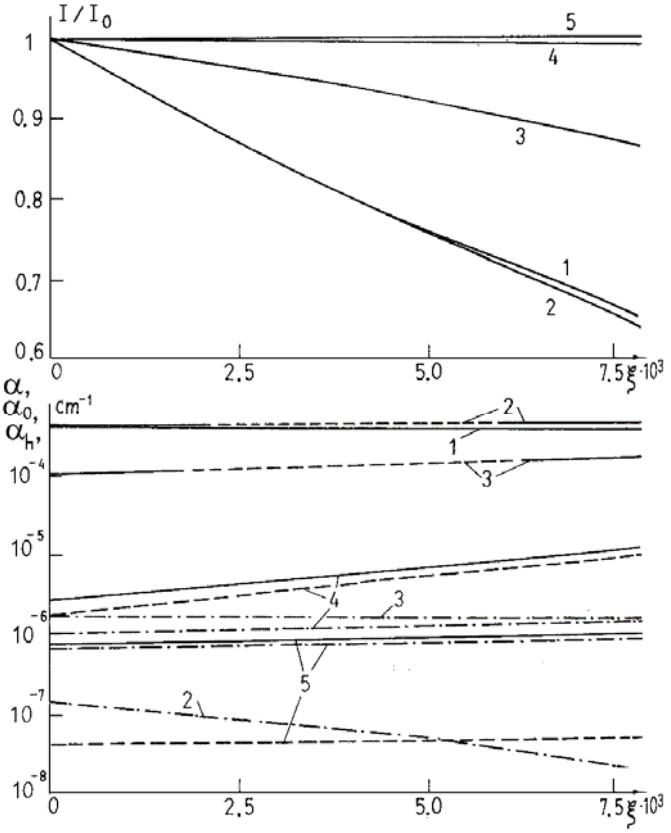

FIG. 3. The distributions of the normalized radiation intensity I/I_0 and the radiation attenuation coefficients of the aerosol medium a (solid lines), the particles α_0 (dashed lines), and the thermal and mass halos around the particles α_h (dot-dashed lines), calculated with $N_0 = 10^2$ cm^{-3} for different times (s): 0 (1); $1.5 \cdot 10^{-4}$ (2); $7.5 \cdot 10^{-4}$ (3); $1.5 \cdot 10^{-3}$ (4); and $2 \cdot 10^{-3}$ (5).

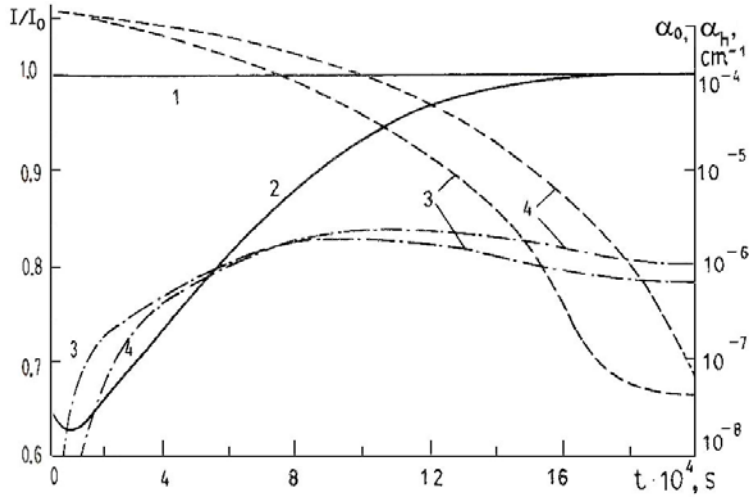

FIG. 4. The time dependences of the pulse intensity $I_0(t)$ (1), transmission of the aerosol layer T_λ with $\varepsilon_\lambda = 7.85 \cdot 10^{-3}$ (2) and the attenuation coefficients of the particles α_h (dashed lines), thermal and mass halos α_h (dot-dashed lines) at the points $\xi = 0$ (3) and $7.85 \cdot 10^{-3}$(4) with $N_0 = 10^2$ cm^{-3}.

Figure 3 shows the distributions of the normalized intensity of the radiation I/I_0 and the attenuation coefficients of the aerosol medium α, the particles α_0, and the thermal and mass halos around the particles α_h over ξ for several times. In the process of heating and melting, resulting in an increase of the particle sizes, taking into account the dependence of the optical parameters on T_0 (Ref. 11) and the appearance of scattering thermal and mass halos around the particles, the radiation attenuation coefficient of the particles increases, and $\alpha \approx \alpha_0$ and $\alpha_h \leq \alpha_0$. This results in some darkening of the aerosol medium under the action of the radiation up to the moment $t = 1.5 \cdot 10^{-4}$ s. The darkening of a solid-particle aerosol under the action of a radiation pulse with $t_p = 1 \cdot 10^{-3}$ s, $\lambda = 1.06$ μm, and moderate energy densities, not resulting in vaporization of the particles, was established experimentally[5] and is explained by the appearance of thermal halos around the particles. As follows from our results, the increase in the particle sizes accompanying melting and the temperature dependence of the optical parameters of the particle material strongly affect the increase in the radiation attenuation coefficient of the aerosol medium.

With the further passage of time, for $t > 1.5 \cdot 10^{-4}$ s, owing to intense vaporization of the particles and growth of the thermal and mass halos α_0 decreases and α_h increases in the entire volume of the aerosol (see Fig. 4). By the moment $t = 1 \cdot 10^{-3}$ s α_h reaches its maximum value, after which it decreases in the entire aerosol layer owing to the appearance of regions with $n < n_0$ in the thermal and mass halos. As a result of the fact that ρ_0 decreases rapidly because of the vaporization of the particles the coefficient a becomes less than α_h, and in addition by the time $t = 2 \cdot 10^{-3}$ s $\alpha \approx \alpha_h$ and $\alpha_0 \ll \alpha_h$.

Figure 4 shows the time dependence of the transmission $T_\lambda = I(\xi_1)/I_0$ of the aerosol layer for $E_0 = 6 \cdot 10^3$ J/cm^2, $t_p = 2 \cdot 10^{-3}$ s. The character of the behavior of the attenuation coefficient α as a function of t, established in this work, results in the fact that T_λ is time dependent and the square shape of the radiation pulse is altered at the outlet from the layer.

REFERENCES

1. V.E. Zuev, Yu.D. Kopytin, and A.V. Kuzikovskii, *Nonlinear Optical Effects in Aerosols* (Nauka, Novosibirsk, 1980).
2. V.E. Zuev, A.A. Zemlyanov, Yu.D. Kopytin, and A.V. Kuzikovskii, *High-Power Laser Radiation in an Atmospheric Aerosol* (Nauka, Novosibirsk, 1984).
3. N.N. Belov, N.P. Datskevich, E.K. Karlova, et al., Zh. Tekh. Fiz. **49**, 333 (1979).
4. V.K. Pustovalov and D.S. Bobuchenko, *Nonlinear Interaction of High-Power Laser Radiation with a Solid Aerosol,* 17, Barnaul, (1986).
5. V.K. Pustovalov and D.S. Bobuchenko, Int. J. Heat and Mass Transfer, **32**, 3 (1989).
6. N.V. Vargaftik, *Handbook of the Thermophysical Properties of Gases and Liquids* (Nauka, Moscow, 1972).
7. C.W. Allen, *Astrophysical Quantities*, The Athlone Press, London (1973) [Russian, translation, Mir, Moscow (1977)].
8. A.A. Radtsig and B.M. Smirnov, *Handbook of Atomic and Molecular Physics* (Atomizdat, Moscow, 1980).
9. N.E. Drits [Ed.], *Handbook of the Properties of the Elements* (Metallurgiya, Moscow, 1985).
10. L.G. Astaf'eva, A.P. Prishivalko, and S.T. Leiko in: *Abstracts of Reports at the All-Union Conference on the Propagation of Laser Radiation in a Dispersed Medium,* Obninsk – Barnaul, **2**, 219 (1988).
11. V.I. Konov and V.N. Tokarev, Kvant. Electron. **10**, 327 (1983).
12. N.N. Belov, Zh. Prikl. Spectrosk., **44**, 948 (1986).
13. V.I. Bukatyi, Inzh,-fiz. zh. **55**, 409 (1988).
14. V.S. Loskutov and G.M. Strelkov, *Propagation of a Laser Pulse in a Soot Aerosol*, Institute of Radio Electronics, Academy of Sciences of the USSR, Preprint No. 24, Moscow (1981).
15. S.V. Zacharchenko, S.D. Pinchuk, and A. R Skripkin, Kvant. Electron. **5**, 934 (1978).